### Title
Handheld spatial frequency domain spectrographic imager for depth-sensitive, quantitative spectroscopy of skin tissue




### ISBN
9781510605152



### Authors
Saager, Rolf B
Dang, An N
Huang, Samantha S
et al.



### Publication Date
2017-02-17

### DOI
10.1117/12.2252518

# Handheld Spatial Frequency Domain Spectrographic Imager for depth-sensitive, quantitative spectroscopy of skin tissue

Rolf B Saager[1*], An N Dang[1], Samantha S Huang[1], Kristen M. Kelly[1,2], Anthony J Durkin[1]
[1]University of California, Irvine, Beckman Laser Institute and Medical Clinic, 1002 Health Sciences Road East, Irvine, California 92612, United States, [2]University of California, Irvine, Department of Dermatology, 118 Medical Surge 1, Irvine, California 92697, United States
[*]rsaager@uci.edu

## ABSTRACT

Here we present a handheld, implementation of Spatial Frequency Domain Spectroscopy (SFDS) that employs line imaging. The new instrument can measure 1088 spatial locations that span a 3 cm line as opposed to our benchtop system that only collects a single 1 mm diameter spot. This imager, however, retains the spectral resolution (~ 1 nm) and range (450 to 1000 nm) of our benchtop system. The device also has tremendously improved mobility and portability, allowing for greater ease of use in clinical setting. A smaller size also enables access to different tissue locations, which increases the flexibility of the device. The design of this portable system not only enables SFDS to be used in clinical settings, but also enables visualization of properties of layered tissues such as skin.

## I. INTRODUCTION

Biological tissues, such as skin, contain a variety of physiological properties that can be probed non-invasively by light. Chemical constituents present in tissue, such as oxygenated and deoxygenated hemoglobin, melanin, lipids, carotenoids, and water can absorb light at differential energies, producing a distinct spectral signature across both visible and near infrared regimes. Light can also elastically scatter off of sub-cellular (e.g. nuclei and mitochondria) and extra-cellular structures (e.g. collagen), where the size and orientation of these structure can influence the tortuous paths photons travel through the tissue. Techniques based on models of light transport in tissue have been developed to extract and isolate the effects of tissue absorption and scattering and thereby quantify functional parameters (hemoglobin concentrations, melanin concentration, etc) and gain some insight in to the bulk structural organization of the tissue.[1] These techniques may be deployed in a variety of measurement geometries ranging from probe-based point spectroscopy to wide-field imaging approaches and utilize a number of illumination/detection schema to exploit temporal and/or spatial responses from light interactions with tissue[2-6].

At the Beckman Laser Institute, we have developed a novel quantitative spectroscopic method that exploits the differential response from absorbing and scattering objects when structured patterns illuminate the tissue[7]. Spatial Frequency Domain Spectroscopy (SFDS) interrogates tissue with a series of sinusoidal intensity patterns and detects the remitted light over a range of 450-1050nm with ~1nm spectral resolution. Absorption and scattering will differentially alter these patterns as light interacts with tissue and subsequently remitted; describing a unique trend in the tissue reflectance as the spatial frequency of these patterns increase. Using inverse solution methods of models of light transport (MC, DA, etc), it has been shown repeatedly in both simulation and experiment that a unique pair of absorption and reduced scattering coefficients can be extracted from these reflectance trends without any spectral constraints on either chromophores present in tissue or wavelength dependent scattering behavior.

As this technique can quantify the absorption and scattering properties in both visible and near-infrared regimes, SFDS can also estimate the depth each wavelength interrogated in tissue[8,9]. This allows SFDS to interpret every part of the measured spectrum in terms of the volume of tissue it interrogated. This is uniquely advantageous, as 1) skin is a highly structured, layered tissue; 2) the typical depth penetrance of visible light is on the order of 100's microns, while near-infrared is on the order of millimeters. Exploiting this opportunity, we have developed a semi-empirical method to estimate chromophore concentrations in skin as a function of depth via a two layer model that leverages the differential depth penetrance between visible and near infrared light.[10] This model has been validated in vivo in terms of its ability to estimate melanin concentration and epidermal thickness across skin types I-VI on the Fitzpatrick Scale[11], as well as its ability to minimize crosstalk from melanin in the estimation of underlying hemodynamics[12].

Photonics in Dermatology and Plastic Surgery, edited by Bernard Choi, Haishan Zeng, Proc. of SPIE
Vol. 10037, 1003703 · © 2017 SPIE · CCC code: 1605-7422/17/$18 · doi: 10.1117/12.2252518

In this paper, we present a new compact instrument design that exploits the quantitative spectroscopic attributes of previous SFDS *in vivo* studies, however executes this technique through a compact, handheld imaging system that introduces spatial imaging capabilities along a single lateral dimension. We discuss the design and fabrication of this new instrument. The performance of this device will also be compared to that of the previous benchtop point-spectroscopy system in terms of 1) independently characterized tissue simulating phantoms to validate the accuracy and fidelity of the SFDS system and 2) an *in vivo* measurement of a benign pigmented lesion to illustrate the application of this technique in a clinical context.

## II. INSTRUMENT DEVELOPMENT

### A. System design Criteria

The primary emphasis on the design of this SFDS imaging system is that it 1) is compact and portable, enabling better clinical utility, 2) collects data along one spatial dimension (line imaging), while 3) maintaining the spectral range and resolution (450-1050nm with ~1nm spectral resolution) of our benchtop, point spectroscopy system. These three objectives translate to a number of specific design criteria when considering the selection of hardware components and the device assembly.

### B. System Description

#### a. Illumination/Projection Unit

In order to provide broadband illumination, we have selected a 150W Quartz Tungsten Halogen light source (Model 21DC, Techniquip). While this unit is relatively large (18x20x10.5cm), is designed to couple light into a fiber bundle or liquid light guide. We have chosen to have this unit stored on a cart and have a 2 meter long liquid light guide (77639, Newport) deliver the broadband light to the handheld imaging head.

We selected an Optoma Pico-Projector for our compact projection unit as it utilizes a digital mirco-mirror device (DMD), which has been the basis of the majority of SFDI instruments[6,7,13-16]. It is an off-the-shelf commercial "pocket projector" with physical dimensions of 3x8x12 cm and a cost of ~$150-300. In contrast, our benchtop system uses a research-grade DMD-based projection unit (GFM) with a size of 12x7x20cm and a cost of ~$10-15k.

As a commercial product intended for projecting computer screens over large distances and fields of view, the Optoma projector requires several modifications before it can be used in a SFDS instrument. The projector uses RGB LEDs, while SFDS requires a broadband illumination. In order to convert the projector to project light spanning 450-1000nm, the Red and Green LEDs are removed along with their respective dichroic mirrors (figure 1). (The Blue LED is covered and kept in the system because it also serves as an interlock for the system firmware operation.) An insertion slot is carved out of the plastic housing to introduce a liquid light guide for the broadband light source and secure it into the same position where the red LED was housed. With this modification to the optical light path, broadband illumination can be directed through the remaining optical components of the projector with minimal stray light losses.

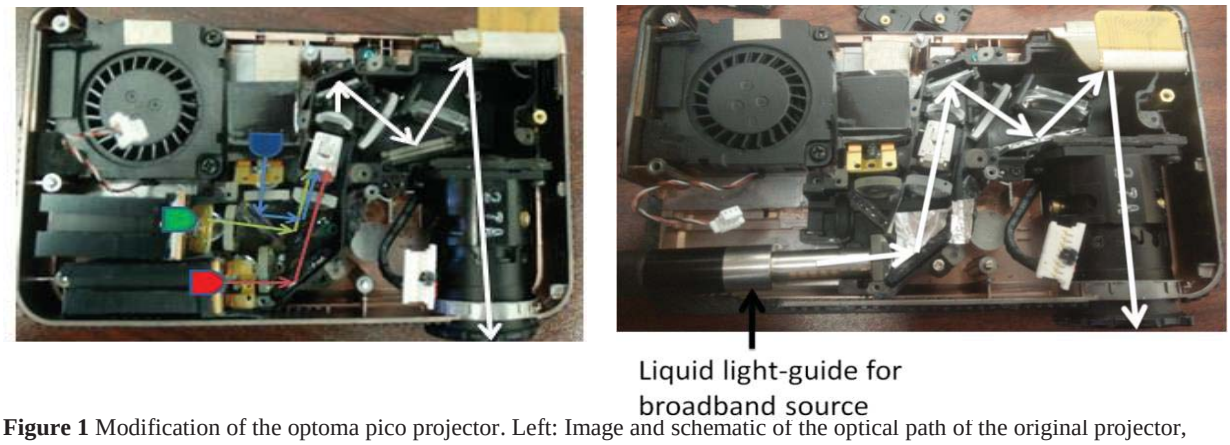


**Figure 1** Modification of the optoma pico projector. Left: Image and schematic of the optical path of the original projector, Right: Image and schematic of the modifications to the optical path. Here the red and green LEDS are removed (the blue LED also serves as a system interlock, so it was left in place but blocked by black electrical tape). Dichroic mirror that combine the green and blue LEDs with the red LED were removed and a liquid light guide, delivering broadband light was inserted into the red LED light path.

Another modification to this "pocket projector" was to reduce the working distance and field of view of the native projection optics. Inserting a 100mm focal length field lens at the distal end of the projection lens system resulted in a 39mm field of view and a working distance of 65 mm.

Additionally, video projections do not display images linearly across the dynamic range of the DMD, rather they are tailored to the nonlinear response of human perception and hence will convolve any input image with a gamma function, before projecting it[17]. We have characterized this nonlinear response function for this specific projector by measuring the intensity of a series of grayscale planar images off of a known reflectance standard (Labsphere) and used this measured function to precondition every spatial frequency image used.

**b. Detection Unit**

A compact line-imaging spectrometer (ImgSpec, Bayspec Inc) was selected to serve as a means to detect the diffusely reflected light from the illuminated tissue. This spectrograph is a ruggedized unit with dimensions of ~22x6x6cm and weighs approximately 5lb. It utilizes a transmission grating that covers a range of 400-1100nm and a large format (1") CMOS sensor as the detector. With an entrance slit of 14.2mmX30micron, the resulting spectral resolution on the 2048x1088 pixel sensor is ~1nm. Relative to the spectrometer used in the benchtop system (Oriel 4770), this compact unit shares an equivalent spectral range and resolution. The Bayspec Imager, however, can acquire 1088 spatial locations simultaneously by imaging the vertical dimension of the 14.2 mm tall slit, while the Oriel only performs point spectroscopy.

Integrating the imaging spectrometer into a handheld system with the modified projector also required some custom mounting components and minor modifications to the unit. To achieve a target Field of View and working distance of ~30 mm and 150mm, respectively via the 35mm Vis/NIR Fixed Focal Length C-Mount lens (#67-716, Edmund Optics) provided with the unit, a 1mm brass spacer was added to the C-Mount thread to modify back focal plane between entrance slit and lens system.

**c. Device Construction**

This portable system was designed with two particular sub components in mind: a handheld imaging head and a small cart (not shown) to house the light source, laptop and uninterruptable power supply. This cart also houses a "holster" for the imaging head to ensure that it is not accidentally dropped when not in use. Between components that permanently reside on the cart and the imager, there is a 2 meter umbilical that connects all power, USB and optical cables.

Handheld Imager (optical head) assembly is shown in figure 3. All optical components are mounted off of a single aluminum base plate (6.4x30x0.3cm). The methods that these specific components are mounted to this base plate are described below.

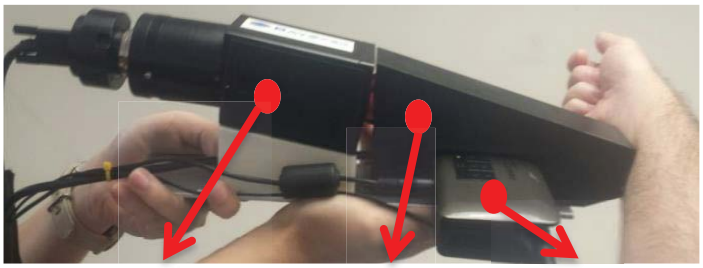


**Figure 3** Clinical Imaging head showing the relative mounting of the imaging spectrograph with respect to the projector and instrument nose cone.

The projector was designed with a single ¼-20 mounting thread at its base. Through this thread, the projector is mounted directly to the aluminum base plate. This, however, only secures the projector to the base plate at a single point. To prevent any rotational misalignment of the projector, the nosecone of this system (described in more detail below) was designed to fit securely over the projection unit. The nosecone is secured to the base plate at four locations (2 in front and 2 behind the projector), thereby securing the projector in a fixed location and orientation.

Angled mounting brackets were fabricated via 3D printing with an 8 degree pitch. These brackets are secured by two 8-32 screws (each) to the base plate and the top of the brackets also align with the four mounting 8-32 tapped mounts at the base of the imaging spectrograph. Offset from the projector, these mounting brackets allows the imaging spectrometer to collect an image at a plane that is not only coincident with the projector's image plane, but given the bracket's height and angle, centered in the projector's field of view.

### d. Webcam

As this spectroscopy system only acquires data along a line, it is difficult to identify where the data is being collected from the tissue. To that end an external imaging component has been added to this instrument. A simple generic webcam, stripped of its commercial housing, has been place next to the projection optics of this device. Matching the working distance of the projection optics, this webcam can provide a 3-color image of tissue across the fields of view of both the projector and spectral imager. With both projector and spectral imager having a fixed, co-planar field of view, the webcam can overlay the precise location of where the imager collects the spectral data in relation to the region of tissue illuminated by the projector. At the start of every acquisition, this webcam image (with the software overlay of the spectral imager data collection) is automatically saved, providing a documented reference of where the data was collected.

## III. SYSTEM EVALUATION

In order to validate the accuracy and performance of this handheld quantitative imaging system, its measurements were first directly compared with an existing, benchtop point-spectroscopy SFDS system in the context of homogeneous tissue simulating phantoms. The objective of this assessment is to demonstrate that the two instruments are spectrally equivalent in terms of bulk optical properties, independent of any depth sensitivity differences due to slight changes in measurement geometry.

In order to demonstrate both the spatial resolution and *in vivo* utility of the line imaging configuration, an example pigmented lesion was imaged. Though clinically benign, this example demonstrates that this imager is capable to measuring a wide range of spatially-resolved optical properties, while maintaining sufficient dynamic range along both spatial and spectral dimensions. Additionally, as skin is a layered tissue, this comparison also indicates whether the measurement geometry of this new imager will be biased toward more superficial or deeper volumes of tissue, relative to the benchtop system.

### A. Comparison using homogeneous tissue phantom

To validate the performance of this handheld SFDS imager to accurately measure the spectral response from turbid media as a function of the spatial frequency used, we compared it to our benchtop system. The comparison was done by using homogeneous tissue phantoms[18]. For this investigation, we used a phantom that used nigrosin as the absorbing agent and titanium oxide as the scattering agent. As nigrosin has strong absorption in the visible but falls off in the Near Infrared, it provides us with the opportunity to cover the broad range of absorption values anticipated in skin in a single medium. With these phantoms, there is no spatial variance in the absorption and scattering properties; therefore, there would not be a difference between using a point spectrometer and a line spectrometer.

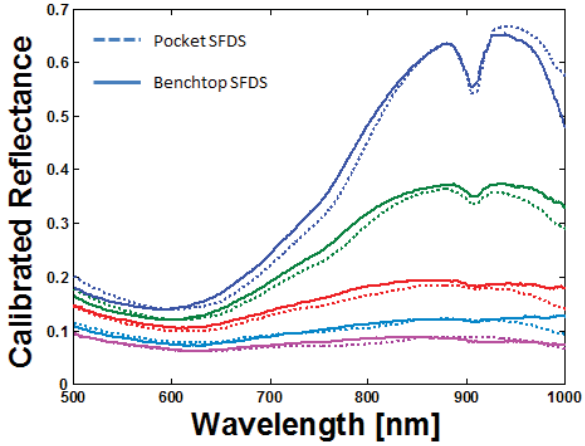


**Figure 4** Calibrated reflectance spectra from a nigrosin tissue simulating phantom at five spatial frequencies. The blue spectra are measured at 0mm$^{-1}$ spatial frequency (i.e. planar illumination) and the magenta spectra are measured at 0.2mm$^{-1}$. Dotted lines are the mean spectra from the handheld imager; solid lines are from the benchtop system.

The two systems were set to have the same spatial frequencies (0, 0.05, 0.1, 0.15, 0.2mm$^{-1}$), phases (0, 120, 240). All data were processed using the same method. Figure 4 shows the calibrated reflectance at all five spatial frequencies measured by both systems. Differences between the two instruments were within 1% agreement. This resulted in differences in the calculated absorption coefficient of <5%, on average. The difference between the calculated reduced scattering coefficient was <2%. The largest spectral differences were observed in over the shortest (450-500nm) and longest (950-1000nm) wavelength bands. These also were the regions where there was the weakest signal detected by both systems. As the 450-500nm region held more than a 10% disparity in absorption between systems, we have opted to only consider >500nm data, as that can be reliably assessed. Although there was also weak signals in the 950-1000nm, the disparity in absorption between instruments remained below 10%.

## IV. DISCUSSION

We have designed and evaluated a handheld SFDS system utilizing commercially available components. This novel, clinic-friendly imager enables *in vivo* study of a wide array of skin pathologies, such as melanoma, burns and wound healing. Our testing and validation have demonstrated that this instrument is equivalent to our benchtop system. It can project any number of spatial frequencies ranging from 0 to 0.5 $mm^{-1}$, with a spectral resolution of ~1 nm. The calibrated reflectance from known tissue simulating phantoms is within ~1% to those measured by the benchtop system, indicating that the calibrated spectral responses of the two systems are equivalent. The agreement between both systems in the context of measuring both normal skin and a benign pigmented lesion indicates that the measurement geometry of both systems covers the same depth of tissue.

The clinical system has a number of advantages over the benchtop system, such as, superior mobility and portability, simultaneous measurement of 1088 spatial locations, and it does all that only at half the cost of the benchtop system. From the in vivo example, it also demonstrates that the clinical imager has sufficient dynamic range to measure both lightly and heavily pigmented tissue, simultaneously. These improvements give the handheld SFDS imager a greater ease of use in clinical setting, allowing access to more patients.

This new instrument is not without limitations. The main disadvantage of this imager is the limited light throughput due to the 30 micron slit of the compact imaging spectrograph. This results in integration times on the order of 15-30 seconds. This limited light throughput issue could be mitigated by replacing the entrance slit of spectrograph with a wider slit, trading off spectral resolution for light throughput. The spectral resolution this current slit provides is, however, preferred in the initial investigational studies planned for this instrument.

## V. CONCLUSION

We have developed a translational, research-grade imager that is compact, quickly implemented and easily deployed in multiple environments. The device now enables investigational studies that are quantitative, depth specific and spatially resolved. This is a critical foundation to gain a better understanding of the morphology and biochemistry of melanoma skin cancers in terms of optically accessible sources of contrast.

## VI. ACKNOWLEDGEMENTS

We thankfully recognize support from the Beckman Foundation and the NIH, including P41EB015890 (A Biomedical Technology Resource) from NIBIB. The content is solely the responsibility of the authors and does not necessarily represent the official views of the NIBIB or NIH. In addition, *this material is based, in-part, upon work supported by the Air Force Office of Scientific Research under award number* ***FA9550-14-1-0034****. Any opinions, finding, and conclusions or recommendations expressed in this material are those of the author(s) and do not necessarily reflect the views of the United States Air Force.* Finally, the purchase of hardware components was supported in part with funding provided under a *UC Irvine, Institute for Clinical and Translational Science Triumvirate grant.*

1. Mourant, J.R., J.P. Freyer, A.H. Hielscher, A.A. Eick, D. Shen, and T.M. Johnson, *Mechanisms of light scattering from biological cells relevant to noninvasive optical-tissue diagnostics.* Appl Opt, 1998. **37**(16): p. 3586-93.
2. Jonasson, H., I. Fredriksson, M. Larsson, and T. Stromberg, *Assessment of the Microcirculation Using Combined Model Based Diffuse Reflectance Spectroscopy and Laser Doppler Flowmetry.* 16th Nordic-Baltic Conference on Biomedical Engineering, 2015. **48**: p. 52-54.
3. Milanic, M., A. Bjorgan, M. Larsson, P. Marraccini, T. Stromberg, and L. Randeberg, *Hyperspectral imaging for detection of cholesterol in human skin.* Optical Diagnostics and Sensing Xv: Toward Point-of-Care Diagnostics, 2015. **9332**.
4. Lo, J.Y., B. Yu, T.F. Kuech, and N. Ramanujam, *A compact, cost-effective diffuse reflectance spectroscopic imaging system for quantitative tissue absorption and scattering.* Advanced Biomedical and Clinical Diagnostic Systems Ix, 2011. **7890**.

5. Liu, J., A. Li, A.E. Cerussi, and B.J. Tromberg, *Parametric Diffuse Optical Imaging in Reflectance Geometry.* Ieee Journal of Selected Topics in Quantum Electronics, 2010. **16**(3): p. 555-564.
6. Cuccia, D.J., F. Bevilacqua, A.J. Durkin, F.R. Ayers, and B.J. Tromberg, *Quantitation and mapping of tissue optical properties using modulated imaging.* J Biomed Opt, 2009. **14**(2): p. 024012.
7. Saager, R.B., D.J. Cuccia, and A.J. Durkin, *Determination of optical properties of turbid media spanning visible and near-infrared regimes via spatially modulated quantitative spectroscopy.* Journal of Biomedical Optics, 2010. **15**(1).
8. Carp, S.A., S.A. Prahl, and V. Venugopalan, *Radiative transport in the delta-P1 approximation: accuracy of fluence rate and optical penetration depth predictions in turbid semi-infinite media.* J Biomed Opt, 2004. **9**(3): p. 632-47.
9. Jacques, S.L. *Optics of light dosimetry for PDT in superficial lesions versus bulky tumors*. 2002. SPIE.
10. Saager, R.B., A. Truong, D.J. Cuccia, and A.J. Durkin, *Method for depth-resolved quantitation of optical properties in layered media using spatially modulated quantitative spectroscopy.* Journal of Biomedical Optics, 2011. **16**(7).
11. Saager, R.B., M. Balu, V. Crosignani, A. Sharif, A.J. Durkin, K.M. Kelly, and B.J. Tromberg, *In vivo measurements of cutaneous melanin across spatial scales: using multiphoton microscopy and spatial frequency domain spectroscopy.* Journal of Biomedical Optics, 2015. **20**(6).
12. Saager, R.B., A. Sharif, K.M. Kelly, and A.J. Durkin, *In vivo isolation of the effects of melanin from underlying hemodynamics across skin types using spatial frequency domain spectroscopy.* Journal of Biomedical Optics, 2016. **21**(5).
13. Rohrbach, D.J., D. Muffoletto, J. Huihui, R. Saager, K. Keymel, A. Paquette, J. Morgan, N. Zeitouni, and U. Sunar, *Preoperative Mapping of Nonmelanoma Skin Cancer Using Spatial Frequency Domain and Ultrasound Imaging.* Academic Radiology, 2014. **21**(2): p. 263-270.
14. Nadeau, K.P., T.B. Rice, A.J. Durkin, and B.J. Tromberg, *Multifrequency synthesis and extraction using square wave projection patterns for quantitative tissue imaging.* Journal of Biomedical Optics, 2015. **20**(11).
15. Lin, A.J., A. Ponticorvo, S.D. Konecky, H.T. Cui, T.B. Rice, B. Choi, A.J. Durkin, and B.J. Tromberg, *Visible spatial frequency domain imaging with a digital light microprojector.* Journal of Biomedical Optics, 2013. **18**(9).
16. Saager, R.B., D.J. Cuccia, S. Saggesse, K.M. Kelly, and A.J. Durkin, *A Led Based Imaging System for Optimization of Photodynamic Therapy of Basal Cell Carcinoma.* Lasers in Surgery and Medicine, 2011. **43**: p. 917-917.
17. Poynton, C.A., *Digital video and HDTV : algorithms and interfaces*. Morgan Kaufmann series in computer graphics and geometric modeling2003, Amsterdam ; Boston: Morgan Kaufmann Publishers. xlii, 692 p.
18. Ayers, F., A. Grant, D. Kuo, D.J. Cuccia, and A.J. Durkin, *Fabrication and characterization of silicone-based tissue phantoms with tunable optical properties in the visible and near infrared domain - art. no. 687007.* Design and Performance Validation of Phantoms Used in Conjunction with Optical Measurements of Tissue, 2008. **6870**: p. 87007-87007.